Available online at www.sciencedirect.com
ScienceDirect
Journal of Sound and Vibration 316 (2008) 50–68
JOURNAL OF SOUND AND VIBRATION
www.elsevier.com/locate/jsvi

A new model for the prediction of turbofan noise with the effect of locally and non-locally reacting liners

Xiaofeng Sun*, Xiaoyu Wang, Lin Du, Xiaodong Jing

School of Jet Propulsion, Beijing University of Aeronautics and Astronautics, 37 Xueyuan Road, Beijing 100083, China

Received 4 September 2007; received in revised form 17 February 2008; accepted 22 February 2008
Handling Editor: L.G. Tham
Available online 11 April 2008

Abstract

This paper presents a unified model to study the effect of both locally and non-locally reacting liners on the sound radiation generated by fan blade rotating sources. This model is set up by the following steps. First, the spinning mode eigenfunction expansions are used to obtain the solution of sound field inside the duct, while the effect of duct liner is modeled by distributed monopole sources, thus effectively avoiding the solution of a difficult complex eigenvalue problem. Secondly, in order to avoid the estimation of the generalized impedances at the inlet and exhaust planes, a boundary element method is used to give the solution outside the duct. With the suitable boundary conditions imposed on the inlet and exhaust planes, a matrix equation is obtained, and the relevant numerical calculation shows this model can not only give a good agreement with existing results for locally reacting liner but also has a capability to predict the sound radiation from fan rotating blade sources with an arbitrary combination of locally and non-locally reacting liners.

1. Introduction

Acoustic treatment in aeroengine nacelle is an essential part of the overall aircraft noise reduction effort. Especially with the increase of bypass ratio of civil transport turbofans, the contribution of fan to the overall noise will be further enhanced [1]. Therefore, the optimization of acoustic treatment and its passive/active control have become a serious concern of aeroacoustician. In fact, considerable work has been done for the prediction of the sound radiation from a lined duct over the last decade, including the boundary integral method or boundary element methods [2,3], the finite element methods [4,5] and the numerical simulation method based on CAA technique [6–9]. It is noted that these methods are playing a diverse role in the different stage of the acoustic design. For the determination of final design parameters, it is necessary to use the numerical simulation tools as accurate as possible to check the results provided the relevant computing cost is affordable. However, for the purpose of preliminary design considerations, an acoustic engineer must conduct a large number of parametric studies. In this situation, the boundary integral methods [2,3] have in fact

*Corresponding author. Tel./fax: +86 10 82317408
E-mail addresses: sunxf@buaa.edu.cn (X. Sun), bhwxy@sjp.buaa.edu.cn (X. Wang), buaaglost@eyou.com (L. Du), jingxd@buaa.edu.cn (X. Jing).

0022-460X/$ - see front matter © 2008 Elsevier Ltd. All rights reserved.
doi:10.1016/j.jsv.2008.02.053

Nomenclature

c_0	sound speed
$f_s(x, y)$	duct cross-section
G	Green's function in the duct $f_s(x, y)$
G'	Green's function in the cavity
h_t	thickness of perforated screen
J_m	Bessel function of the first kind of order m
J'_m	first derivative of J_m
k_0	wavenumber
$k_{m,n}$	radial wavenumber of mode (m, n)
m	spinning mode order
M	Mach number of uniform flow
p	acoustic pressure
p_0	mean pressure
p_d	disturbance acoustic pressure in a duct with locally reacting liners
p_d^+	disturbance acoustic pressure in the liner cavity
p_d^-	disturbance acoustic pressure in a duct with non-locally reacting liners
p_i	acoustic pressure of incident sound wave
r_0	radius of duct
r_s	radial coordinate of spinning point dipoles
$\vec{r}$	vector coordinate
$\vec{r}'$	vector coordinate denotes the mass source singularities
r, φ, z	cylindrical coordinates
$s(\vec{r})$	duct wall surface
T	thrust of spinning point dipoles
x, y, z	orthogonal coordinates
Z	specific admittance ratio
α	source term
δ_{jk}	$\begin{cases} 1 & (j=k) \\ 0 & (j\neq k) \end{cases}$
ϕ	eigenfunction of a solid circular duct
Φ	eigenfunction of a solid duct
$\gamma_{m,n}^{\pm}$	axial wavenumber of mode (m, n)
η	compliance of perforated screen
μ, n	radial mode order
ρ	acoustic density
ρ_0	mean density
τ	time associated with emission of sound wave; time delay
ω	angular frequency
ξ	amplitude of the particle displacement

become one of the fast, useful and reliable tools. In addition, this method has also been extended to study the optimization design of acoustic treatments [10] and the active control technique [11]. Therefore, any further development for this kind of method may still be required for the practical application point of view.

In the development of the boundary integral methods, Myers and Kosanchik III [3] presented a model to predict the sound radiation with the effect of both rotating source and lined duct based on solving the linearized Ffcowcs Williams–Hawkings equation. An alternative method was suggested by Dunn et al. [2] using potential theory. In particular, the latter includes the capability of handling arbitrary liner distributions inside the duct, and it is thus more suitable for the optimizing design of multi-segmented liners. On the other hand, it is suggested that future acoustic liners may consist of hybrid active–passive elements in many current investigations, which possess not only the advantages of a conventional liner but also the capability to adjust the acoustic impedance of liner to adapt to the changing aeroengine environment. It is also noted that non-locally reacting liner has more design degrees of freedom than locally reacting liner, which has generally two degrees of freedom, i.e. the liner thickness (cavity depth) and the resistance of the perforated plate. It is thus believed that non-locally reacting liner may play an important role in the future noise suppressor design of turbofans. Especially, a kind of non-locally reacting liner with the adjustable wall impedance using bias flow has long been receiving great attention with the emphasis on both the mechanism related to sound absorption and possible applications [12–22]. However, for a non-locally reacting liner, the effect of the liner cannot be described as the impedance boundary condition anymore because acoustic waves in the liner also propagate parallel to the wall. Therefore, any effective description for this situation must contain simultaneously the solution of the acoustic fields both inside and outside the liner. It is obvious that the existing boundary integral method will not be suitable for this problem. Naturally, if aiming at the parametric study of future advanced liner, it is necessary to develop a model to include the effect of both locally and non-locally reacting liners on the prediction of sound radiation from ducted rotating blade sources.

In this investigation, we present a unified model to study the effect of both locally and non-locally reacting liners on the sound radiation. This model is set up by the following three steps. First, we still use the spinning mode eigenfunction expansions to obtain the solution of sound field inside the duct [23,24], while the effect of duct liner is modeled by monopole sources suggested by Namba and Fukushige [25], which effectively avoids the solution of a difficult complex eigenvalue problem. In particular, the singularity treatment in the Namba's method has been replaced by a novel approach, which suggests to study a new kind of noise suppressor related to membrane vibration by Huang [26]. In addition, after describing the acoustic field inside the liner using Green's function theory, the present model can also be extended to handle the non-locally reacting liner. Secondly, considering the eigenfunctions still meet the orthogonal condition in our case, we construct a solution for a given lined duct element with arbitrarily axial length and position, which has the interface parameters as unknown variables. For this particular process, we have in fact extended the solution for an infinitely long duct with finite acoustic treatment length to that for a finite length duct element without calculating the complex eigenvalues for the softwall. It is found that it is particularly useful to construct such an element solution so that to make full use of the existing mode-match technique [24]. Thirdly, in order to avoid the estimation of the generalized impedances at the inlet and exhaust planes [27,28], a boundary element method is suggested to give the solution outside the duct [29–31]. With the suitable boundary conditions imposed on the inlet and exhaust planes, we can obtain a matrix equation which includes the unknown variables both inside and outside the acoustic fields.

In the following sections, we will first describe the theoretical details mentioned as above for this model, and then introduce how to construct various transfer elements for both locally and non-locally reacting liners. Especially, emphasis is also placed on how to match the solution inside the duct with the acoustic field outside the duct through the boundary element method, which naturally results in a matrix equation. Finally, various examples are presented to check if the results are correct or not. In fact, for locally reacting liners the present model gives a good agreement with the existing results. On the other hand, it is noted that this model also provides some interesting results for non-locally reacting liners. In particular, we have shown the possibility of controlling the sound propagation in a lined duct with bias flow.

2. Analytical model

2.1. Basic solution for a finite domain in ducts with locally reacting liner

As shown in Fig. 1, a duct of arbitrary uniform cross-section is considered here, in which a uniform mean flow is contained. Now, we discuss how to solve the acoustic field in a domain from $z = 0$ to l with an impedance wall. By applying the Green's function theory, Zorumski [24] verified that the solution in the domain could be written in the form of

$$p_m = \sum_{n=1}^{N} [B_n \Phi(k_{m,n} r) e^{i\gamma^-_{m,n} z} + C_n \Phi(k_{m,n} r) e^{i\gamma^+_{m,n}(z-l)}], \tag{1}$$

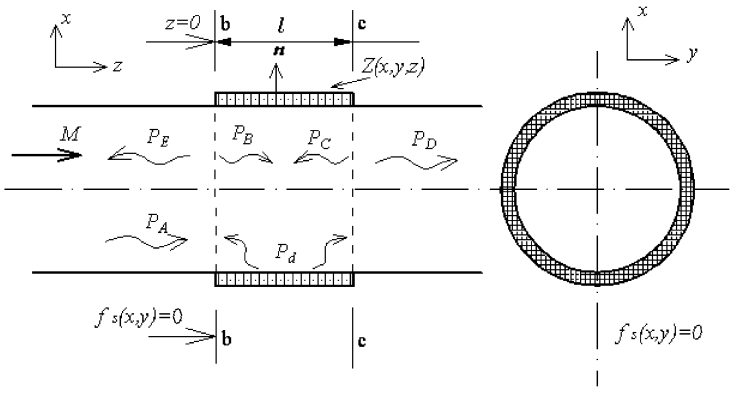

Fig. 1. Geometry of an infinite duct with arbitrary cross-section.

where m and n represent the circumferential and radial mode number, respectively, while $k_{m,n}$ is the radial eigenvalue obtained by satisfying the impedance boundary condition. It is noted that a close matrix equation with modal coefficient B_n and C_n as unknown variables can be obtained by imposing the mass and momentum conservations on the interfaces. This work was called "mode-matching method", which was widely applied to the optimizing design for multi-segmented liners. However, as we have mentioned in the Introduction, the difficulty arising from the eigenvalue computation limits its further application. In addition, for a flow duct, it can be verified that the eigenfunction $\Phi(k_{m,n}r)$ does not satisfy the orthogonality anymore [24], which may also affect the accuracy and convergence of the computing results.

In order to overcome these difficulties, Namba and Fukushige [25] showed that the effect of a liner could be modeled as monopoles with unknown source strength, which naturally avoids the calculation of complex eigenvalues. In fact, the numerical results from this model reveal an excellent agreement with those obtained by using Wiener–Hopf technique [32]. However, this model only remains valid for an infinitely long rectangular duct and needs to handle various singularities appeared in the integral equation. Therefore, in order to form the solution similar to Eq. (1), the key to the problem lies in how to solve the integral equation for a finite domain by making use of the same basic assumptions suggested in Ref. [25]. For this reason, we are trying to construct the solution by the following steps.

Now, we define the cross-section of the duct as $f_s(x, y) = 0$. The mean flow is assumed to be with pressure p_0, density ρ_0, speed of sound c_0, and Mach number M. The wall of the duct is lined with a locally reacting acoustic liner of specific acoustic impedance Z. Incident sound source is assumed to be located at $z = -\infty$. Positive or negative Mach number $M(M<1)$ means downstream or upstream propagation of uniform flow, respectively. Assuming the effects of viscosity and heat transfer negligible, we have

$$\frac{1}{c_0^2}\frac{D_0^2 p}{D\tau^2} - \nabla^2 p = \alpha(\vec{r}', \tau), \tag{2}$$

where $D_0/Dt = (\partial/\partial t) + U(\partial/\partial z)$, $U = Mc_0$, $\alpha(\vec{r}', \tau)$ represents the source term. To solve the sound field in the duct, the acoustic pressure p in the domain can be regarded as a sum of an undisturbed incident acoustic pressure component p_i and a disturbance pressure component p_d, i.e.

$$p = p_i + p_d. \tag{3}$$

The incident acoustic pressure p_i is defined as the pressure that would be realized if the wall of the duct is entirely hard. Then p_i must satisfy the wall boundary condition

$$\frac{\partial p_i}{\partial n} = 0 \quad \text{for} \quad \vec{r} \quad \text{on} \quad f_s(x, y) = 0. \tag{4}$$

For simplicity, in most of the computational models, the incident acoustic wave p_i are usually treated as a single mode coming from one direction, which interacts directly with the scattering object. However, superposition principle for a liner system states that a linear combination of solutions to a linear equation is again a solution of the liner system, so, we can directly consider the incident waves interacting with the liner shown in Fig. 1 with the following expression:

$$p_i = p_B + p_C = \sum_{\mu=1}^{N} [B_\mu \Phi_{m,\mu}(x, y)\, e^{i\gamma^-_{m,\mu} z} + C_\mu \Phi_{m,\mu}(x, y)\, e^{i\gamma^+_{m,\mu}(z-l)}], \tag{5}$$

where

$$\gamma^{\pm}_{m,\mu} = \begin{cases} \dfrac{Mk_0}{\beta^2} + \dfrac{\kappa_{\mu,m}}{\beta^2} & \text{for upstream,} \\ \dfrac{Mk_0}{\beta^2} - \dfrac{\kappa_{\mu,m}}{\beta^2} & \text{for downstream,} \end{cases} \tag{6}$$

$$\kappa_{\mu,m} = \begin{cases} \sqrt{k_0^2 - \beta^2 k_{m,\mu}^2} & k_0^2 > \beta^2 k_{m,\mu}^2, \\ -\mathrm{i}\sqrt{\beta^2 k_{m,\mu}^2 - k_0^2} & k_0^2 < \beta^2 k_{m,\mu}^2, \end{cases} \tag{7}$$

$$\beta^2 = \sqrt{1 - M^2}, \quad k_0 = \omega/c_0, \tag{8}$$

where $k_{m,\mu}$ denotes the eigenvalue with the condition of solid wall. On the other hand, for a monopole source, we can apply the Generalized Green's function method [33] to obtain its solution in the form of

$$\tilde{p}_d(\vec{r}, t) = -\int_{-T}^{T} \int_{s(\tau)} \rho_0 \tilde{V}'_n \frac{D_0 G}{D\tau} \, \mathrm{d}s(\vec{r}') \, \mathrm{d}\tau, \tag{9}$$

where $\tilde{V}'_n$ is the velocity normal to the liner surface, while Green's function can be expressed as

$$G = \frac{-\mathrm{i}}{4\pi} \sum_{m=-\infty}^{\infty} \sum_{\mu=1}^{\infty} \frac{\Phi_{m,\mu}(x,y)\Phi^*_{m,\mu}(x',y')}{\Gamma_{m,\mu}} \int_{-\infty}^{\infty} \frac{1}{\kappa_{\mu,m}} \mathrm{e}^{\mathrm{i}\omega(t-\tau)+\mathrm{i}\gamma^{\pm}_{m,\mu}(z-z')} \, \mathrm{d}\omega. \tag{10}$$

Substituting Eq. (10) into Eq. (9) yields

$$\tilde{p}_d = p_d \, \mathrm{e}^{\mathrm{i}\omega t} = \frac{\rho_0 \, \mathrm{e}^{\mathrm{i}\omega t}}{2} \sum_{m=-\infty}^{\infty} \sum_{\mu=1}^{\infty} \frac{\Phi_{m,\mu}(x,y)}{\Gamma_{m,\mu}} \int_{s(\tau)} V'_n \Phi^*_{m,\mu}(x',y') \frac{[\omega + U\gamma^{\pm}_{m,\mu}]}{\kappa_{\mu,m}} \mathrm{e}^{\mathrm{i}\gamma^{\pm}_{m,\mu}(z-z')} \, \mathrm{d}s(\vec{r}'), \tag{11}$$

where

$$\int_A \Phi_m \Phi^*_n \, \mathrm{d}x \, \mathrm{d}y = \begin{cases} 0 & (m \neq n), \\ \Gamma_n & (m = n). \end{cases} \tag{12}$$

At the surface of the liner, p_i, p_d and Z must satisfy the boundary condition

$$\frac{p}{-V_n} = Z, \tag{13}$$

due to Eq. (3), it can be rewritten as

$$p_d + ZV_n = -p_i, \tag{14}$$

where V_n is acoustic particle velocity, by the application of displacement continuity condition, V'_n can be expressed as

$$V'_n = \frac{\partial \xi}{\partial \tau} + U \frac{\partial \xi}{\partial z'} = V_n + \frac{U}{\mathrm{i}\omega} \frac{\partial V_n}{\partial z'}. \tag{15}$$

Eq. (14) is actually an integral equation with unknown sources strength related to V_n. The solution of this equation generally needs to handle various singularities as introduced in Goldstein and Namba's works [25,33]. In order to avoid this difficulty, we can manipulate Eq. (14) in a different way [26], letting V_n be expanded into the form

$$V_n = \sum_{k=1}^{\infty} V_k(x',y') \sin \frac{k\pi z'}{l}. \tag{16}$$

Substituting Eq. (16) into Eq. (15), we thus have

$$V'_n = \left(1 + \frac{U}{\mathrm{i}\omega} \frac{\partial}{\partial z'}\right) V_n = \left(1 + \frac{U}{\mathrm{i}\omega} \frac{\partial}{\partial z'}\right) \sum_{k=1}^{\infty} V_k \sin \frac{k\pi z'}{l}. \tag{17}$$

The Fourier sine transform of Eq. (14) in the region $0 < z < l$ is

$$\frac{2}{l} \int_0^l p_d \sin \frac{j\pi z}{l} \, \mathrm{d}z + \frac{2}{l} \int_0^l Z V_n \sin \frac{j\pi z}{l} \, \mathrm{d}z = -\frac{2}{l} \int_0^l p_i \sin \frac{j\pi z}{l} \, \mathrm{d}z. \tag{18}$$

Substituting Eqs. (16) and (17) into Eq. (11) and then taking Fourier sine transforming of Eq. (11) in the region $0<z<l$, it is verified that

$$\frac{2}{l}\int_0^l p_d \sin\frac{j\pi z}{l}\,\mathrm{d}z = \sum_{k=1}^{\infty} z_{jk} V_k, \quad j = 1,2,3,\ldots, \tag{19}$$

where

$$z_{jk} = \frac{\rho_0}{l}\sum_{m=-\infty}^{\infty}\sum_{n=1}^{\infty}\frac{\Phi_{m,n}(x,y)}{\Gamma_{m,n}} \times \int_0^l\int_{s(\tau)}\frac{[\omega+U\gamma_{m,n}^{\pm}]}{\kappa_{n,m}}\Phi_{m,n}^{*}(x',y')\,\mathrm{e}^{\mathrm{i}\gamma_{mn}^{\pm}(z-z')}\left(1+\frac{U}{\mathrm{i}\omega}\frac{\partial}{\partial z'}\right)\sin\frac{k\pi z'}{l}\mathrm{d}s(\vec{r'})\sin\frac{j\pi z}{l}\,\mathrm{d}z. \tag{20}$$

Then Eq. (14) can be rewritten as

$$\sum_{k=1}^{\infty}(z_{jk}+\delta_{jk}Z)V_k = -I_j, \quad j = 1,2,3,\ldots, \tag{21}$$

where

$$I_j = \frac{2}{l}\int_0^l\sum_{\mu=1}^{N}[B_\mu\Phi_{m,\mu}(x,y)\,\mathrm{e}^{\mathrm{i}\gamma_{m,\mu}^{-}(z)} + C_\mu\Phi_{m,\mu}(x,y)\,\mathrm{e}^{\mathrm{i}\gamma_{m,\mu}^{+}(z-l)}]\sin\frac{j\pi z}{l}\,\mathrm{d}z = \sum_{\mu=1}^{N}\Phi_{m,\mu}(x,y)[B_\mu I_j^{B_\mu} + C_\mu I_j^{C_\mu}]. \tag{22}$$

For circumferential mode m, using mode-matching condition yields

$$V_k = \sum_j (z_{jk}+\delta_{jk}Z)^{-1} I_j = \sum_j \Im_{jk}^{-1} I_j. \tag{23}$$

As we have seen, I_j contains unknown coefficients B_μ and C_μ. According to superposition principle of linear waves and Eqs. (11), (17), (22) and (23), the scattering field can be expressed as

$$p_d = \sum_{n=1}^{N} p_{dn}\Phi_{m,n}(x,y) = \frac{\rho_0}{2}\sum_{n=1}^{N}\frac{\Phi_{m,n}(x,y)\,\mathrm{e}^{\mathrm{i}\gamma_{m,n}^{\pm}z}}{\Gamma_{m,n}}\left\{\sum_{\mu=1}^{\infty}\left[B_\mu Q_{n\pm}^{B_\mu} + C_\mu Q_{n\pm}^{C_\mu}\right]\right\}, \tag{24}$$

where

$$Q_{n\pm}^{B_\mu} = \sum_{k=1}^{M_0}\sum_j \Im_{jk,\mu,B_\mu}^{-1} I_j^{B_\mu} S_k^{n\pm}\Phi_{m,\mu}(x,y), \quad Q_{n\pm}^{C_\mu} = \sum_{k=1}^{M_0}\sum_j \Im_{jk,\mu,C_\mu}^{-1} I_j^{C_\mu} S_k^{n\pm}\Phi_{m,\mu}(x,y) \quad f_s(x,y) = 0,$$

$$S_k^{n\pm} = \int_s \Phi_{m,n}^{*}(x',y')\frac{[\omega+U\gamma_{m,n}^{\pm}]}{\kappa_{n,m}}\,\mathrm{e}^{-\mathrm{i}\gamma_{m,n}^{\pm}z'}\left(1+\frac{U}{\mathrm{i}\omega}\frac{\partial}{\partial z'}\right)\sin\frac{k\pi z'}{l}\,\mathrm{d}s(\vec{r'}). \tag{25}$$

As a specific example, we can use the present method to construct a close matrix equation to obtain the solution for an infinitely long duct described in Fig. 1. In fact, with the interface $z=0$ or l as a relative coordinate, the sound propagation in a different direction can be described as

$$p_A = \sum_{n=1}^{N} A_n\Phi_{m,n}(x,y)\,\mathrm{e}^{\mathrm{i}\gamma_{m,n}^{-}z}, \tag{26}$$

$$p_B = \sum_{n=1}^{N} B_n\Phi_{m,n}(x,y)\,\mathrm{e}^{\mathrm{i}\gamma_{m,n}^{-}z}, \tag{27}$$

$$p_C = \sum_{n=1}^{N} C_n\Phi_{m,n}(x,y)\,\mathrm{e}^{\mathrm{i}\gamma_{m,n}^{+}(z-l)}, \tag{28}$$

$$p_D = \sum_{n=1}^{N} D_n \Phi_{m,n}(x,y)\, \mathrm{e}^{\mathrm{i}\gamma^-_{m,n}(z-l)}, \tag{29}$$

$$p_E = \sum_{n=1}^{N} E_n \Phi_{m,n}(x,y)\, \mathrm{e}^{\mathrm{i}\gamma^+_{m,n} z}. \tag{30}$$

All these waves are composed of modal components that can be specified by the notation (m, n). In addition, the known source p_A is assumed to locate at $z = -\infty$, and only the cut-on modes are considered. On the other hand, once the unknown coefficients B_n, C_n, D_n, E_n $(n = 1, 2, 3, \ldots, N)$ are determined, the corresponding acoustic field in the duct can be obtained through Eqs. (26)–(30). To illustrate how to solve the coefficients, an infinite circular duct with uniform cross-section model is considered here, i.e., $\Phi_{m,n}(x,y) = \phi_m(k_{m,n}r)\,\mathrm{e}^{\mathrm{i}m\varphi}$. Eqs. (24) and (26–30) imply that, to describe the sound field in the duct, $4N$ unknown coefficients (B_n, C_n, D_n, E_n) have to be determined. According to the pressure and axial velocity continuity conditions on the cross-section $b-b$ and $c-c$, we have

$$\begin{aligned} p^-_b &= p^+_b, \quad v^-_{bz} = v^+_{bz} \\ p^-_c &= p^+_c, \quad v^-_{cz} = v^+_{cz}. \end{aligned} \tag{31}$$

Substituting Eqs. (24)–(30) into Eq. (31) yields

$$\begin{aligned}
&\sum_n E_n\phi_m(k_{m,n}r) + \sum_n A_n\phi_m(k_{m,n}r) = \sum_n (B_n + C_n\,\mathrm{e}^{-\mathrm{i}\gamma^+_{m,n}l})\phi_m(k_{m,n}r) + \sum_n p_{dn}\phi_m(k_{m,n}r),\\
&\sum_n \frac{E_n\gamma^+_{m,n}\phi_m(k_{m,n}r)}{\omega + U\gamma^+_{m,n}} + \sum_n \frac{A_n\gamma^-_{m,n}\phi_m(k_{m,n}r)}{\omega + U\gamma^-_{m,n}}\\
&\quad = \sum_n \left(\frac{B_n\gamma^-_{m,n}}{\omega + U\gamma^-_{m,n}} + \frac{C_n\gamma^+_{m,n}\,\mathrm{e}^{-\mathrm{i}\gamma^+_{m,n}l}}{\omega + U\gamma^+_{m,n}} \right)\phi_m(k_{m,n}r) + \sum_n \frac{\gamma^+_{m,n}p_{dn}\phi_m(k_{m,n}r)}{\omega + U\gamma^+_{m,n}},\\
&\sum_n (B_n\,\mathrm{e}^{\mathrm{i}\gamma^-_{m,n}l} + C_n)\phi_m(k_{m,n}r) + \sum_n p_{dn}\,\mathrm{e}^{\mathrm{i}\gamma^-_{m,n}l}\phi_m(k_{m,n}r) = \sum_n D_n\phi_m(k_{m,n}r),\\
&\sum_n \left(\frac{\gamma^-_{m,n}B_n\,\mathrm{e}^{\mathrm{i}\gamma^-_{mn}l}}{\omega + U\gamma^-_{m,n}} + \frac{C_n\gamma^+_{m,n}}{\omega + U\gamma^+_{m,n}} \right)\phi_m(k_{m,n}r) + \sum_n \frac{p_{dn}\gamma^-_{m,n}\,\mathrm{e}^{\mathrm{i}\gamma^-_{m,n}l}}{\omega + U\gamma^-_{m,n}}\phi_m(k_{m,n}r)\\
&\quad = \sum_n \frac{D_n\gamma^-_{m,n}\phi_m(k_{m,n}r)}{\omega + U\gamma^-_{m,n}}, \quad n = 1, 2, 3, \ldots, N.
\end{aligned} \tag{32}$$

Since the eigenfunction ϕ_m satisfy orthogonality, the simultaneous algebraic equations can be written as

$$\begin{cases}
E_n - B_n - C_n\,\mathrm{e}^{-\mathrm{i}\gamma^+_{m,n}l} - p_{dn} = -A_n\\
\dfrac{\gamma^+_{m,n}}{\omega + U\gamma^+_{m,n}}E_n - \dfrac{\gamma^-_{m,n}}{\omega + U\gamma^-_{m,n}}B_n - \dfrac{\gamma^+_{m,n}\,\mathrm{e}^{-\mathrm{i}\gamma^+_{m,n}l}}{\omega + U\gamma^+_{m,n}}C_n - \dfrac{\gamma^+_{m,n}}{\omega + U\gamma^+_{m,n}}p_{dn} = -\dfrac{\gamma^-_{m,n}}{\omega + U\gamma^-_{m,n}}A_n\\
B_n\mathrm{e}^{\mathrm{i}\gamma^-_{m,n}l} + C_n + p_{dn}\mathrm{e}^{\mathrm{i}\gamma^-_{m,n}l} - D_n = 0\\
\dfrac{\gamma^-_{m,n}\,\mathrm{e}^{\mathrm{i}\gamma^-_{m,n}l}}{\omega + U\gamma^-_{m,n}}B_n + \dfrac{\gamma^+_{m,n}}{\omega + U\gamma^+_{m,n}}C_n + \dfrac{\gamma^-_{m,n}\,\mathrm{e}^{\mathrm{i}\gamma^-_{m,n}l}}{\omega + U\gamma^-_{m,n}}p_{dn} - \dfrac{\gamma^-_{m,n}}{\omega + U\gamma^-_{m,n}}D_n = 0, \quad n = 1, 2, 3, \ldots, N.
\end{cases} \tag{33}$$

Obviously the coefficients B_n, C_n, D_n, E_n can be determined by solving algebraic Eq. (33). For brevity, Eq. (33) can be simplified as

$$\begin{Bmatrix} ss^1_E & ss^1_B & ss^1_C & 0 \\ ss^2_E & ss^2_B & ss^2_C & 0 \\ 0 & ss^3_B & ss^3_C & ss^3_D \\ 0 & ss^4_B & ss^4_C & ss^4_D \end{Bmatrix} \begin{Bmatrix} p_E \\ p_B \\ p_C \\ p_D \end{Bmatrix} = \begin{Bmatrix} p_A \\ v_A \\ 0 \\ 0 \end{Bmatrix}, \tag{34}$$

where each *ss* denotes a coefficients matrix, for example:

$$ss_B^1 = \begin{bmatrix} -1 & 0 & \cdots & 0 \\ 0 & -1 & \cdots & 0 \\ \vdots & \vdots & \ddots & \vdots \\ 0 & 0 & \cdots & -1 \end{bmatrix} + \begin{bmatrix} -cs_{1+}^{B_1} & -cs_{1+}^{B_2} & \cdots & -cs_{1+}^{B_N} \\ -cs_{2+}^{B_1} & -cs_{2+}^{B_2} & \cdots & -cs_{2+}^{B_N} \\ \vdots & \vdots & \ddots & \vdots \\ -cs_{N+}^{B_1} & -cs_{N+}^{B_2} & \cdots & -cs_{N+}^{B_N} \end{bmatrix}, \tag{35}$$

where $cs_{n+}^{B_\mu} = (\rho_0/2)(e^{i\gamma_{m,n}^+ z}/\Gamma_{m,n})Q_{n+}^{B_\mu}$, and

$$p_A = \overbrace{\{-A_1, -A_2, \ldots, -A_N\}^{\mathrm{T}}}^{N}$$

$$v_A = \overbrace{\left\{-\frac{\gamma_{m,1}^- A_1}{\omega + U\gamma_{m,1}^-}, -\frac{\gamma_{m,2}^- A_2}{\omega + U\gamma_{m,2}^-}, \ldots, -\frac{\gamma_{m,n}^- A_N}{\omega + U\gamma_{m,n}^-}\right\}^{\mathrm{T}}}^{N}. \tag{36}$$

And $\{ss_B^1\}_{N\times N}$ represents a matrix related to the sound wave p_B defined in Eq. (27). Therefore, for each section, the corresponding matrix can be described as

$$\begin{Bmatrix} ss_B^1 & ss_C^1 \\ ss_B^2 & ss_C^2 \\ ss_B^3 & ss_C^3 \\ ss_B^4 & ss_C^4 \end{Bmatrix}_{4n\times 2n}. \tag{37}$$

Up to now, we have derived the solution in a finite domain with the unknown variables on the interfaces. For simplicity, the solution consisting of Eqs. (3), (5) and (24) and the corresponding matrix expression defined in Eq. (37) is called as a "transfer element". More importantly, later on we will see that the solution for non-locally reacting liner can also be expressed as a transfer element, which just remains as the unknown interface parameters. This actually means that for a duct with arbitrary combinations of locally and non-locally reacting liners, its solution of acoustic field can be obtained by the following two steps, firstly dividing the duct into various duct elements with different acoustic treatment configuration as shown in Fig. 2, and then establishing the relation between the transfer elements by imposing suitable conditions on the interface of each element. Compared to the mode-matching method [24], the transfer element we constructed need not require calculating the difficult complex eigenvalues and also need not assume that the wall impedance is piecewise uniform. Furthermore, the eigenfunctions still satisfy orthogonality, which means there is good convergence theoretically. With some combination of different elements, we can carry out various optimizing design for a better sound attenuation in a lined duct. For convenience in the following discussion, we call what is suggested in this investigation as "transfer element method" (shorten by TEM). In fact, it will be

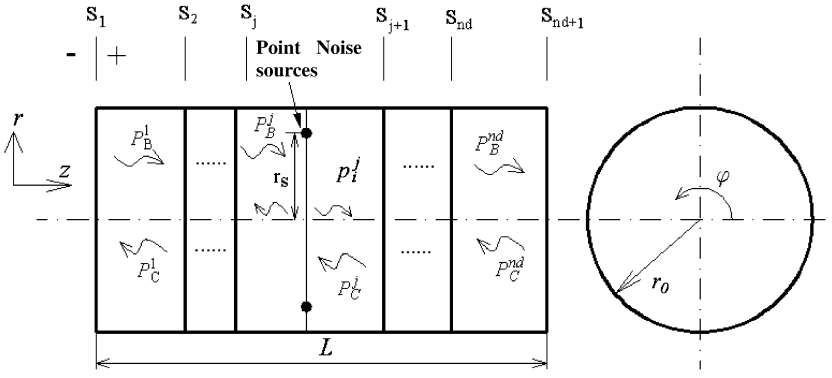

Fig. 2. Geometry of a finite duct with *nd* transfer elements.

demonstrated that by combining TEM with BIEM, sound radiation from a finite length duct can be calculated no matter what kind of liner is distributed on the duct.

2.2. Basic solution for a finite domain in ducts with non-locally reacting liner

The geometry of non-locally reacting liner is showed in Fig. 3. As stated earlier, this kind of perforated liner has been receiving great attention mainly due to its potential for various practical applications [12–22]. In Fig. 3, p_i, p_d^-, and p_d^+ denote incident acoustic pressure, disturbance acoustic pressure in duct and disturbance acoustic pressure in cavity, respectively. For the cavity, its Green's function can be expressed as

$$G' = -\frac{1}{2\pi}\sum_{m=-\infty}^{\infty}\sum_{n=1}^{\infty}\sum_{q=0}^{\infty}\frac{\Phi_{m,n}(x,y)\cos(q\pi z/l)\Phi^*_{m,n}(x',y')\cos(q\pi z'/l)}{\Gamma_{m,n,q}}\int_{-\infty}^{\infty}\frac{e^{i\omega(t-\tau)}}{k_0^2-k_{m,n,q}^2}\,d\omega, \tag{38}$$

where

$$k_{m,n,q}^2 = k_{m,n}^2 + \left(\frac{q\pi}{l}\right)^2, \tag{39}$$

$$\Gamma_{m,n,q} = \int_0^l\int_{A'}\Phi_m(x,y)\Phi_n^*(x',y')\cos\frac{q\pi z}{l}\cos\frac{q\pi z}{l}\,dS(\vec{r'})\,dz = \begin{cases}\Gamma_{m,n}\frac{l}{2} & q\neq 0,\\ \Gamma_{m,n}l & q=0.\end{cases} \tag{40}$$

We thus obtain

$$p_d^+ = i\rho_0\omega\sum_m\sum_n\sum_q\frac{\Phi_{m,n}(x,y)\cos(q\pi z/l)}{\Gamma_{m,n,q}(k_0^2-k_{m,n,q}^2)}\int_{s(\tau)}V_n\Phi^*_{m,n}(x',y')\cos\frac{q\pi z'}{l}\,dS(\vec{r'}). \tag{41}$$

It is noted that p_d^- has the same expression as defined in Eq. (11). As Fig. 3 shows, the acoustic properties of a perforated screen can be described as the compliance related to the Rayleigh conductivity c of a single aperture in a rigid baffle [13–15]. Hughes and Dowling [14] adopted the Rayleigh conductivity of a single aperture in a plane proposed by Howe [13] to construct a smooth compliance for a perforated screen with bias flow. The same procedure will be used in the present study. Due to the boundary condition on the surface of liner, we have

$$p_d^- - p_d^+ + \frac{i\omega\rho_0 Q}{c} = -p_i, \tag{42}$$

i.e.

$$p_d^- - p_d^+ + \frac{i\omega\rho_0 V_n}{\eta} = -p_i, \tag{43}$$

where Q denotes the fluctuating aperture volume flux and η is related to Ref. [21]

$$\frac{1}{\eta} = \frac{\pi a^2}{\sigma}\frac{1}{K_a} + \frac{h_t}{\sigma}, \tag{44}$$

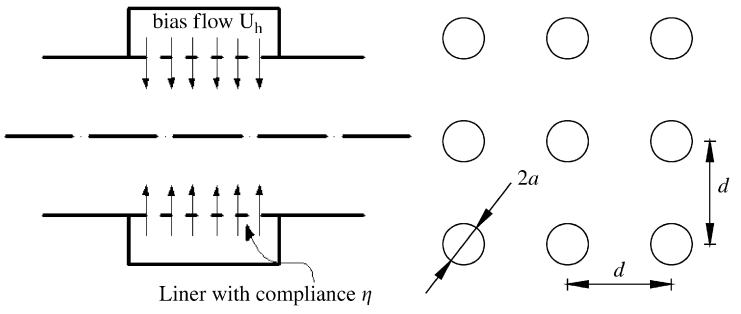

Fig. 3. Geometry of a non-locally reacting liner.

where h_t is the liner thickness and

$$\sigma \equiv \pi a^2/d^2, K_a = 2a(\gamma + \mathrm{i}\delta), \tag{45}$$

where γ and δ are given by Eq. (3.14) of Ref. [13]. Like Eq. (20), the relevant algebraic equations can be written as

$$\sum_k \left(z_{jk}^- - z_{jk}^+ + \delta_{jk} \frac{\mathrm{i}\omega\rho_0}{\eta} \right) V_k = -I_j, \tag{46}$$

where

$$z_{jk}^+ = \frac{2\mathrm{i}\rho_0\omega}{l} \sum_m \sum_n \sum_q \frac{\Phi_{m,n}(x,y)}{\Gamma_{m,n,q}(k_0^2 - k_{m,n,q}^2)} \int_0^l \cos\frac{q\pi z}{l} \int_{s(\tau)} \Phi_{m,n}^*(x',y') \cos\frac{q\pi z'}{l} \sin\frac{k\pi z'}{l} \, \mathrm{d}S(\vec{r'}) \sin\frac{j\pi z}{l} \, \mathrm{d}z, \tag{47}$$

$$z_{jk}^- = z_{jk}. \tag{48}$$

The same procedure as shown in Eq. (20) for a locally reacting liner can be used to solve Eq. (47), i.e., the effect of non-locally reacting liner can also be considered in the present model.

2.3. Sound radiation from a finite duct

To predict sound radiation of a finite duct with uniform cross-section, as Fig. 4 shows, a boundary integral equation method (BIEM) is applied instead of using the mode reflection coefficients defined in Refs. [27,28]. Based on potential theory, the sound radiation of the duct can be obtained by using Eq. (49) when the boundary conditions $p(Q)$, $\partial p(Q)/\partial n$ on the exterior surface are known

$$C(P)p(P) = \int_S \left[p(Q) \frac{\partial G(P,Q)}{\partial n} - \frac{\partial p(Q)}{\partial n} G(P,Q) \right] \mathrm{d}S(Q), \tag{49}$$

here P, Q are points on the surface S, n is outwards normal direction at a point on the surface, p is the surface pressure. The function G is the free-space Green's function $G(P,Q) = \exp(-\mathrm{i}k_0R)/4\pi R$, where $R = |r_p - r_q|$. Depending on the position of P, the value of $C(P)$ is given by

$$C(P) = 1 + \int_S \frac{\partial}{\partial n_q} \left[\frac{1}{4\pi R} \right] \mathrm{d}S(Q). \tag{50}$$

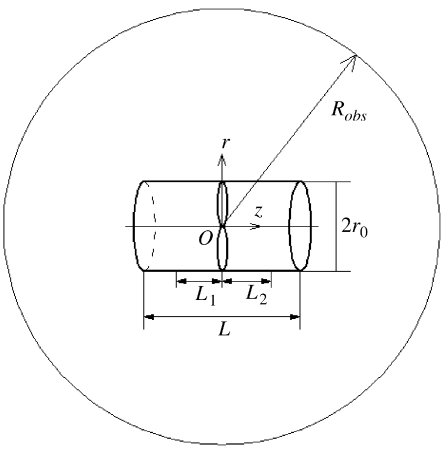

Fig. 4. Geometry of duct and observation point.

Obviously we have

$$\begin{aligned} &C(p) = 0 \quad \text{for} \quad P \quad \text{in duct},\\ &C(p) = 1 \quad \text{for} \quad P \quad \text{out of duct},\\ &C(p) = 0.5 \quad \text{for} \quad P \quad \text{on a smooth surface of duct.} \end{aligned} \tag{51}$$

Considering properties of the axisymmetric duct, and using the expansion of the boundary conditions and the surface distribution functions in Fourier series with respect to the angle of revolution, the surface integral of Eq. (49) is reduced to a line integral along the generator of the duct [29–31]. As suggested in Ref. [31], the evaluation of Eq. (49) can be performed numerically by discretizing the generator of the duct into a series of curvilinear isoparametric elements. As Fig. 5 shows, there are $2M_1 + M_2$ nodes along the generator. Each element has 3 nodes, i.e. $(2M_1 + M_2 - 3)/2$ elements here. Discretizing boundary integral Eq. (49), $2M_1 + M_2$ algebraic equations can be obtained

$$\begin{aligned} &c(P_j)p_{mj} - \sum_{n=1}^{N_e}\sum_{a=1}^{3} p_{mna}A^a_{mnj} + \sum_{n=1}^{N_e}\sum_{a=1}^{3} p^n_{mna}C^a_{mnj} = 0\\ &j = 1, 2, 3, \ldots, 2M_1 + M_2, \quad N_e = 2M_1 + M_2 - 3. \end{aligned} \tag{52}$$

Here, the method mentioned in Ref. [31] is used to obtain the correlative coefficients matrixes A^a_{mnj}, C^a_{mnj}. m denote the circumferential modes of the sound sources, p_{mna} and p^n_{mna} are the values of p, $\partial p/\partial n$ at the ath node of nth element. Obviously, there are $4M_1 + 2M_2$ unknowns in Eq. (52). Because the exterior surface of the duct is assumed to be solid, the values of $\partial p/\partial n$ there must satisfy the boundary condition $\partial p/\partial n = 0$. Then $4M_1 + M_2$ unknowns remain in Eq. (52). To obtain the values of these unknowns, the other $2M_1$ equations need to be constructed.

It should be noted that Eq. (49) is based on Eq. (2), assuming the source term $\alpha(\vec{r}', \tau) = 0$. When there is only z-axis uniform flow, and express the sound pressure as $p = p(x, y, z)e^{i\omega t}$, we can rewrite Eq. (2) as

$$\frac{\partial^2 p}{\partial x^2} + \frac{\partial^2 p}{\partial y^2} + (1 - M^2)\frac{\partial^2 p}{\partial z^2} - 2\frac{i\omega M}{c_0}\frac{\partial p}{\partial z} + k_0^2\ p = 0. \tag{53}$$

Letting $p(x, y, z) = \Psi(x, y, \zeta)\, e^{ik'_0 M\zeta}, k'_0 = k_0/\beta,\ z = \beta\zeta$, Eq. (53) will be rearranged as

$$\frac{\partial^2 \Psi}{\partial x^2} + \frac{\partial^2 \Psi}{\partial y^2} + \frac{\partial^2 \Psi}{\partial \zeta^2} + k'^2_0 \Psi = 0. \tag{54}$$

Eq. (54) is a Helmholtz equation. It can be solved by Eq. (52) to get the values of Ψ, $\partial\Psi/\partial z$. Then the values of p, $\partial p/\partial n$ can be obtained as follows:

$$\frac{\partial p}{\partial n} = \frac{\partial p}{\partial z} = \frac{e^{ik'_0 M\zeta}}{\beta}(\Psi_n + ik'_0 M\Psi) \quad \text{for} \quad Q \quad \text{on} \quad R_{\text{duct}} \quad \text{section}, \tag{55}$$

$$\frac{\partial p}{\partial n} = -\frac{\partial p}{\partial z} = \frac{e^{ik'_0 M\zeta}}{\beta}(-\Psi_n + ik' M\Psi), \quad \text{for} \quad Q \quad \text{on} \quad L_{\text{duct}} \quad \text{section}. \tag{56}$$

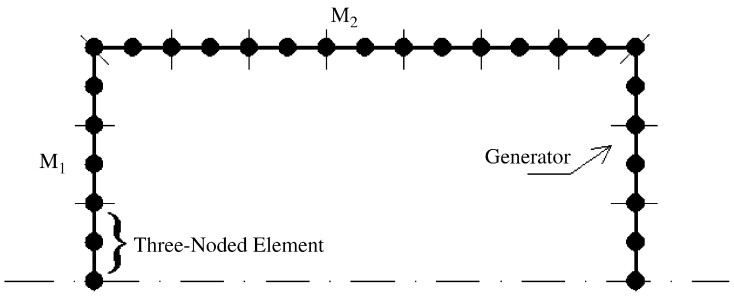

Fig. 5. Typical discretization scheme of the generator of a duct.

It is well known that if the duct is zero thickness, there is a singularity at the leading edge of the duct. To avoid this problem, we assume the duct has a finite thickness h_d, and $h_d \ll r_1$. In spite of this, as an approximation treatment, we still regard the flow both inside and outside the duct as uniform flow. In addition, the Kutta condition is imposed on the trailing edge of the duct during discretizing the equation.

In the present model, the incident sound is produced by a collection of M_s points or line monopoles and/or dipoles. The duct has n_d sections, i.e. n_d+1 cross-sections, as shown Fig. 2, and the interior surface of each section has different boundary conditions. The sound sources are assumed to be located in the jth section. The sound pressure field can be described by

$$p_i^j = \sum_{n=1}^{N} p_{in}^j \phi_m(k_{m,n} r)\, \mathrm{e}^{\mathrm{i}\gamma_{m,n}^- z}, \tag{57}$$

$$p_B^j = \sum_{n=1}^{N} B_n^j \phi_m(k_{m,n} r)\, \mathrm{e}^{\mathrm{i}\gamma_{m,n}^- z}, \tag{58}$$

$$p_C^j = \sum_{n=1}^{N} C_n^j \phi_m(k_{m,n} r)\, \mathrm{e}^{\mathrm{i}\gamma_{m,n}^+ (z-l_j)}, \tag{59}$$

$$p_d^j = \frac{\rho_0}{2} \sum_{n=1}^{N} \frac{\phi_m(k_{m,n} r)\mathrm{e}^{\mathrm{i}\gamma_{m,n}^{\pm} z}}{\Gamma_{m,n}} \left\{ \sum_{\mu=1}^{N} \left[B_\mu^j Q_{n\pm}^{B_\mu} + C_\mu^j Q_{n\pm}^{C_\mu} \right] \right\}, \tag{60}$$

where superscript j denotes the number of the section. N denotes how many radial modes are considered. $\phi_m(k_{m,n}r)$ is the eigenfunction. For a circular duct, $\phi_m(k_{m,n}r)$ should be the first kind Bessel function $J_m(k_{m,n}r)$, where $k_{m,n}$ is the eigenvalue which is given by $J'_m(k_{m,n}r) = 0$. Letting $N = M_1$, from Eqs. (52) and (57)–(60), we know that, (4 + 2nd) $M_1 + M_2$ unknowns have to be determined to describe the whole sound field. Based on TEM, the algebraic equations can be obtained

$$\begin{Bmatrix}
ss_{B_p}^{2-} & ss_{C_p}^{2-} & ss_{B_p}^{2+} & ss_{C_p}^{2+} & & & & & & \\
ss_{B_v}^{2-} & ss_{C_v}^{2-} & ss_{B_v}^{2+} & ss_{C_v}^{2+} & & & & & & \\
 & & ss_{B_p}^{3-} & ss_{C_p}^{3-} & \cdots & & & & & \\
 & & ss_{B_v}^{3-} & ss_{C_v}^{3-} & \cdots & & & & & \\
 & & & & \cdots & ss_{B_p}^{(n_d-1)+} & ss_{C_p}^{(n_d-1)+} & & & \\
 & & & & \cdots & ss_{B_v}^{(n_d-1)+} & ss_{C_v}^{(n_d-1)+} & & & \\
 & & & & & ss_{B_p}^{n_d-} & ss_{C_p}^{n_d-} & ss_{B_p}^{n_d+} & ss_{C_p}^{n_d+} \\
 & & & & & ss_{B_v}^{n_d-} & ss_{C_v}^{n_d-} & ss_{B_v}^{n_d+} & ss_{C_v}^{n_d+}
\end{Bmatrix}_{\substack{2(n_d-1)M_1 \\ \times 2n_d M_1}}
\begin{pmatrix} B^1 \\ C^1 \\ \vdots \\ \vdots \\ \vdots \\ \vdots \\ B^{n_d} \\ C^{n_d} \end{pmatrix}
=
\begin{pmatrix} 0 \\ \vdots \\ pp_i^{n+} \\ vv_i^{n+} \\ pp_i^{(n+1)-} \\ vv_i^{(n+1)-} \\ \vdots \\ 0 \end{pmatrix}_{2(n_d-1)M_1}. \tag{61}$$

The known quantities on the right side are relative to incident waves. Superscript of $ss_{B_p}^{2-}$ denotes on the left side of S_2. As mentioned above, $2M_1 + M_2$ and $2(n_d-1)M_1$ algebraic equations have been obtained by using BIEM and TEM, respectively. Based on the p and $\partial p/\partial n$ continuity conditions on the inlet and outlet cross-section, $4M_1$ can be constructed

$$\begin{Bmatrix}
BB_p^{1-} & AA_{Bp}^{1+} & AA_{Cp}^{1+} & \\
BB_{p^n}^{1-} & AA_{Bp^n}^{1+} & AA_{Cp^n}^{1+} & \\
 & AA_{Bp}^{(nd+1)-} & AA_{Cp}^{(n_d+1)-} & CC_p^{(n_d+1)+} \\
 & AA_{Bp^n}^{(nd+1)-} & AA_{Cp^n}^{(n_d+1)-} & CC_{p^n}^{(n_d+1)+}
\end{Bmatrix}_{4M_1 \times 6M_1}
=
\begin{Bmatrix} pp_{\mathrm{i}p}^{1+} \\ pp_{\mathrm{i}p^n}^{1+} \\ pp_{\mathrm{i}p}^{(n_d+1)-} \\ pp_{\mathrm{i}p^n}^{(n_d+1)-} \end{Bmatrix}_{4M_1 \times 1}, \tag{62}$$

where subscript p, p^n denote that the matrix is relative to p or $\partial p/\partial n$, respectively. Matrix BB and CC are concerning the values of p and $\partial p/\partial n$ of each nodes on the radius. They are defined by

$$\int_0^{r_0} p\phi_m(k_{m,n}r)r\,\mathrm{d}r, \tag{63}$$

$$\int_0^{r_0} \frac{\partial p}{\partial n}\phi_m(k_{m,n}r)r\,\mathrm{d}r. \tag{64}$$

Solving the simultaneous linear equations composed of Eqs. (52), (61) and (62), the $(4+2\mathrm{nd})M_1+M_2$ unknowns will be determined, i.e. the sound boundary condition of the duct can be obtained. It is therefore concluded that the sound radiation from a finite duct can be determined by combining TEM with BIEM, especially including the effect of both locally and non-locally reacting liners.

3. Results and discussions

3.1. Numerical results for a finite length treatment in an infinitely long duct

As a check to the present model, we first need to judge if the solution of a single transfer element described by Eqs. (3), (5), (24) and (37) is correct or not. For this purpose, consider a plane wave coming from $-\infty$, which propagates between the two infinite parallel walls. To study how the wave interacts with a finite length liner from $z=0$ to l shown in Fig. 1, we have two ways to realize the goal. The one way is to let the incident wave directly satisfy the boundary condition on the source surface to obtain the results by solving the corresponding integral equation just like Namba and Fukushige [25] did. The other way is to let the incident wave meet the matching conditions on the interface ($z=0$ or l) described in the present model to obtain the results. For this case, the eigenfunction is

$$\Phi_n = \sqrt{\varepsilon_n}\cos(k_n x), \tag{65}$$

where $x=h=1\,\mathrm{m}$ is the height of the parallel duct and

$$k_n = \frac{n\pi}{h}, \quad \varepsilon_n = \begin{cases} 1 & n=0, \\ 2 & n\neq 0. \end{cases} \tag{66}$$

In addition, the length of liner is $l=4.339\,\mathrm{m}$ and the mean flow is $M=0$. The impedance is given by

$$Z = R + \mathrm{i}\left[\frac{R\omega}{\omega_0} - \cot\left(\frac{\omega d}{c_0}\right)\right], \tag{67}$$

where $R=1.4$, $\omega_0=25.57c_0$, $d=0.271\,\mathrm{m}$. The liner is only placed on the surface of $x=0$. In addition, the sound attenuation shown in Fig. 6 represents the insertion loss between the inlet and outlet planes of the incident wave. From this figure, we see that the results from two different ways agree with each other very well for most of the frequency range. However, there is some derivation for higher non-dimensional frequencies (4–5). As for the present results, we found that the model can provide good convergent results even for higher frequency case. Therefore, the minor deviation in Fig. 6 may come from different methods of solving the integral equation.

The second example is about a two-section locally reacting liner in axial series combination. In this case, Mach number of the mean flow is $M=0.4$. As shown in Fig. 7, the liner is composed of two sections, and $l_1/l=0.5$, $R_1=0.8$, $R_2=0.6$, $\omega_{01}=\omega_{02}=25.86c_0$. Fig. 7 reveals that TEM gives the same results as those published in Ref. [25].

The third example is about a non-locally reacting liner. The comparison is made between our results and those from recent study conducted by Eldredge [22]. The latter was obtained by using Green's function method and boundary value theory of differential equations. Fig. 8 is the schematic related to the computation, and we still use the sound absorption coefficient defined in Ref. [21]. As seen in Fig. 9, the results of TEM agree well with the findings from Eldredge's model for both plane incident wave and higher order mode wave.

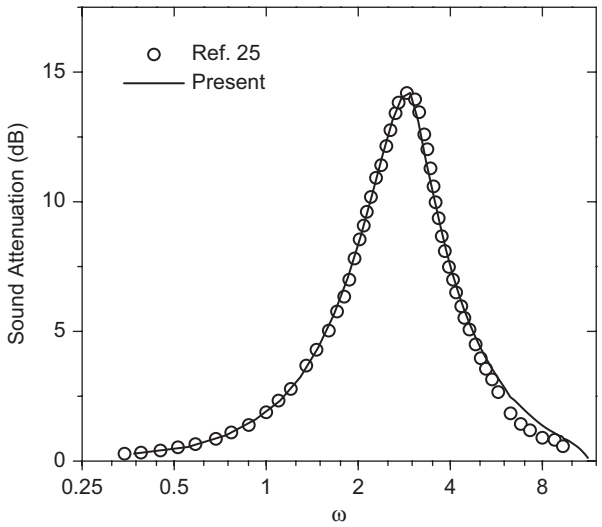

Fig. 6. Sound power attenuation for the fundamental (0, 0) mode incident and a uniform liner. $R = 1.4$, $\omega_0 = 25.5c_0$, $d = 0.271$ m.

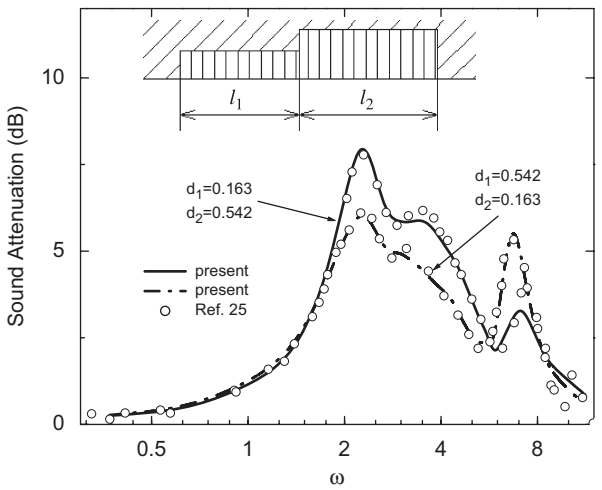

Fig. 7. Effect of liner depths on the sound power attenuation for the fundamental (0, 0) mode incident. $R_1 = 0.8$, $R_2 = 0.6$, $\omega_{01} = \omega_{02} = 25.86c_0$.

It is concluded from the above three examples that TEM can provide that same results as the existing methods for both locally and non-locally reacting liner by only using the interface matching conditions instead of directly satisfying the boundary condition in the lined surface [12,25]. More importantly, if combining TEM with BIEM, we can see that it is possible to compute the sound radiation from a finite length duct containing arbitrary combinations of both locally and non-locally reacting liners.

3.2. Numerical results from a finite duct with various sound sources

For this case, we first make a comparison with Myers' results [34]. A finite duct shown in Fig. 4 is considered here, where O denotes the origin. The length of the duct is L, L_1, L_2 represent the length of liner, respectively. Radius of the duct is r_0. The observation point is on the sphere defined by R_{obs}. A time periodic, distributed but very narrow spherical source is located at O. $L_1 = L_2 = 0$, i.e. all the interior surface of the duct is hard wall. In Ref. [34], the sound source is given in free space. For our case, we need to obtain the expression for an

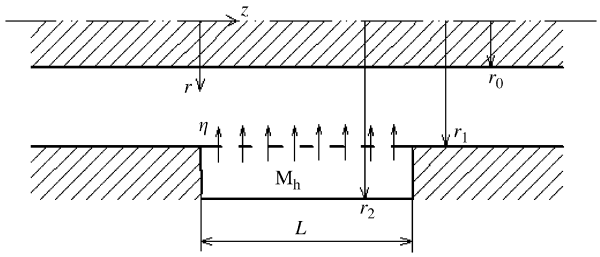

Fig. 8. Geometry of a annular duct with non-locally reacting liner. $L = 1\,\mathrm{m}$, $r_0/L = 0.0282$, $r_1/L = 0.358$, $r_2/r_1 = 1.67$, $\sigma = 0.0398$, $a/L = 2.11 \times 10^{-3}$, $h_t/L = 0.0237$, $M_h = 0.05$, $M = 0$.

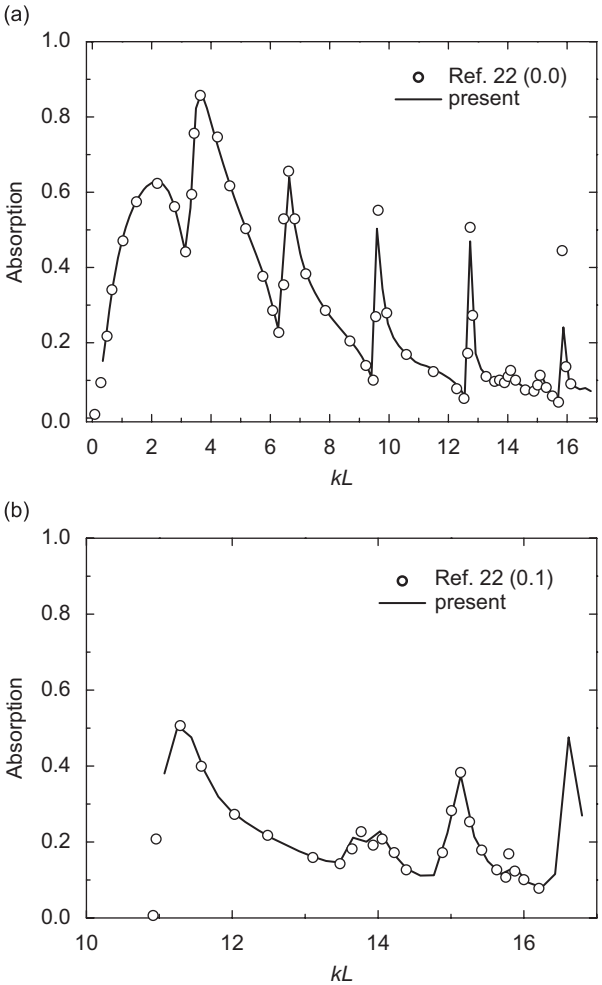

Fig. 9. Absorption of different modes by single non-locally reacting liner.

infinitely long duct. By using the generalized Green's function method [33], the sources in the duct can be described as

$$p_i' = \frac{A\rho_0 e^{i\omega t}}{2} \sum_{n=1}^{\infty} [\omega + U\gamma_{m,n}^{\pm}] \frac{\Phi(k_{m,n}r)}{\Gamma_{m,n}} \frac{e^{i\gamma_{m,n}^{\pm} z}}{\kappa_{n,m}}. \tag{68}$$

As seen in Fig. 10, there is little difference between the two results for both the acoustic directivity and the corresponding amplitude almost at all observation points.

For a rotating source, consider that 20 spinning axial dipoles, situated on a disk in the middle of a short duct, generate the twentieth circumferential mode of acoustic pressure and its harmonics [2,35]. The acoustic field generated by the spinning point axial dipoles sources in our computational model is rewritten as

$$p_i' = \frac{BT\,e^{isB\Omega t}}{2} \sum_{m=-\infty}^{\infty} \sum_{n=1}^{\infty} \frac{\Phi(k_{m,n}r)\Phi(k_{m,n}r_s)}{\Gamma_{m,n}} \frac{\gamma_{m,n}^{\pm}}{\kappa_{n,m}} e^{i\gamma_{m,n}^{\pm} z}, \tag{69}$$

where B denotes the number of blades and also represents the number of dipoles in our computation. The disk is located at the center of the duct. The observation point is located on sphere $R_{obs} = 10\,m$. The result in Fig. 11 is obtained when the duct has solid interior surface. The results of the present method are in a relatively good agreement with those reported in Ref. [35].

Fig. 12 shows the results including the effect of two-section locally reacting liners. As seen in Fig. 12, compared with the results from Ref. [35], the present predictions have almost the same directivity at any observation point but there are certain discrepancies for the amplitude in the inlet of the duct.

The reason for the discrepancies observed in Figs. 10–12 may be explained by the following two aspects, the one is that these results come from different computational methods; and the second is that in order to avoid the leading edge singularity we assume that the duct has a finite thickness instead of being an infinitely thin, which may affect both directivity and amplitude of the sound radiation to a certain extent. Anyway, the results of Figs. 10–12 have in fact demonstrated that TEM and BIEM can be combined to solve the sound scattering problem of a finite lined duct containing rotating sound sources within acceptable accuracy limits.

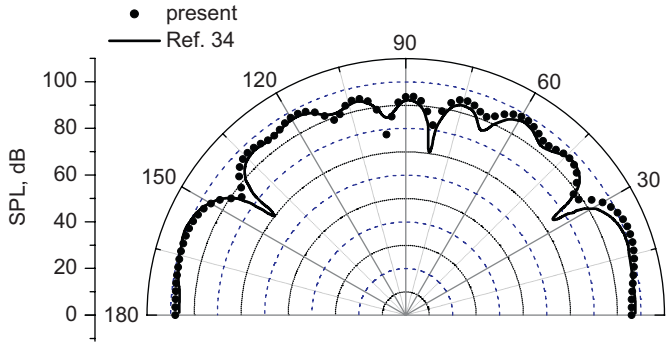

Fig. 10. Sound pressure level at spherical radius 2.5 m; $L = 2\ r_0 = 1\,m$, $M = 0.5$, $\omega r_0/c_0 = 2.2045\pi$, $\rho_0 c_0 A = 1$.

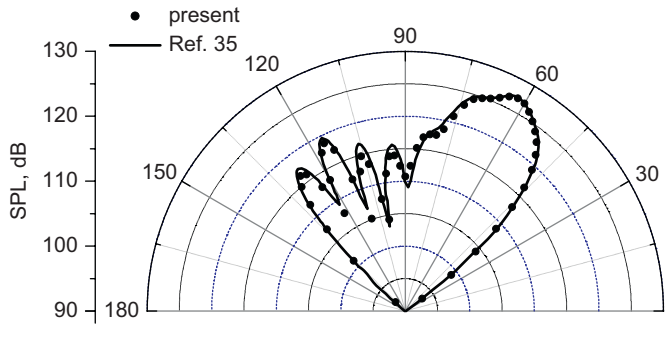

Fig. 11. Sound pressure level at spherical radius 2.5 m; $M = -0.4$, $T = 1.0\,kN$, $\omega r_0/c_0 = 1.22$, $L = r_0 = 1.0\,m$, $r_s/r_0 = 0.9$, $L_1 = L_2 = 0$.

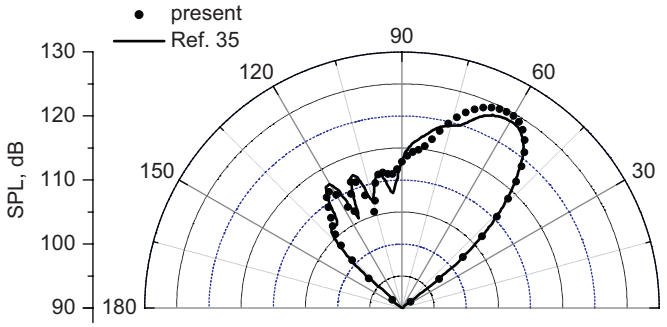

Fig. 12. Sound pressure level at spherical radius 10 m; $M=-0.4$, $T=1.0$ kN, $\omega r_0/c_0=1.22$, $L=r_0=1.0$ m, $r_s/r_0=0.9$, $L_1=L_2=0$, $Z_1=2+0i$, $Z_2=0.5+0.5i$.

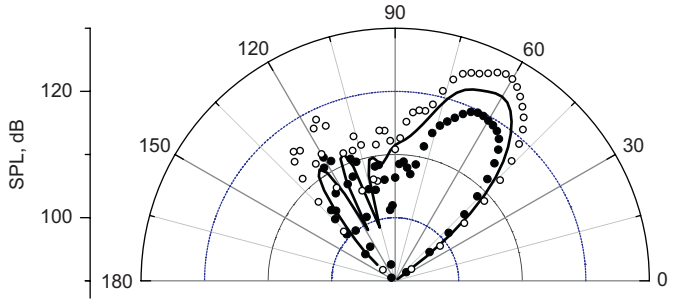

Fig. 13. Sound pressure level at spherical radius 10 m; $M=-0.4$, $T=1.0$ kN, $\omega r_0/c_0=1.22$, $L=r_0=1.0$ m, $r_s/r_0=0.9$, $L_1=L_2=0.4$ m; ○, hard surface; —, locally reacting liner: $Z_1=Z_2=(1.0,\ 1.5)$; ●, non-locally reacting liner; $r_1=1.2$ m, $h_t=0.001$ m, $\sigma=0.02$, $a=0.001$, $M_h=0.023$.

3.3. Effect of non-locally reacting liners

As mentioned above, the present method can be used to calculate the sound radiation from a finite length duct containing arbitrary combinations of both locally and non-locally reacting liners. Fig. 13 is an example for this case. If replacing the locally reacting liner given in Ref. [35] with a non-locally reacting liner having the same length, and giving the input parameters for this liner as shown in Fig. 13, we can first predict the compliance of the screen according to Eqs. (44) and (45), and then the corresponding acoustic fields can be computed. It is found from Fig. 13 that the radiating sound pressure of the duct is decreased effectively in this case compared with the results from the locally reacting liner. However, this does not mean that any non-locally reacting liner has certainly better performance than a locally reacting one if not carefully designing the relevant parameters. Fig. 14 is a schematic of a combination of locally and non-locally reacting liners with the same treatment length. From Fig. 15, it is found that if taking the bias flow $M_h=0.005$, the corresponding sound attenuation represented by hollow circles in Fig. 15 is not as good as that from the pure locally reacting liner at most of the observation points. However, if letting bias flow $M_h=0.05$, the solid circles shown in Fig. 15 stand for the computing results and the attenuation is much better than those from the above two cases. In fact, it has long been known that the properties of a non-locally reacting liner can be altered by adjusting the speed of the bias flow. The reason is the change of resistance and reactance of the perforated plate due to the vortex–sound interaction [14]. However, the computational results given in Fig. 15 also show that a better sound attenuation in a duct may be realized as long as we carefully design the non-locally reacting liner, including the introduction of suitable amount of bias flow. On the other hand, for a different sound source, it is also possible that the corresponding speed of bias flow could be introduced to actively suppress the noise on the basis of our suggestions. It is thus believed that our method

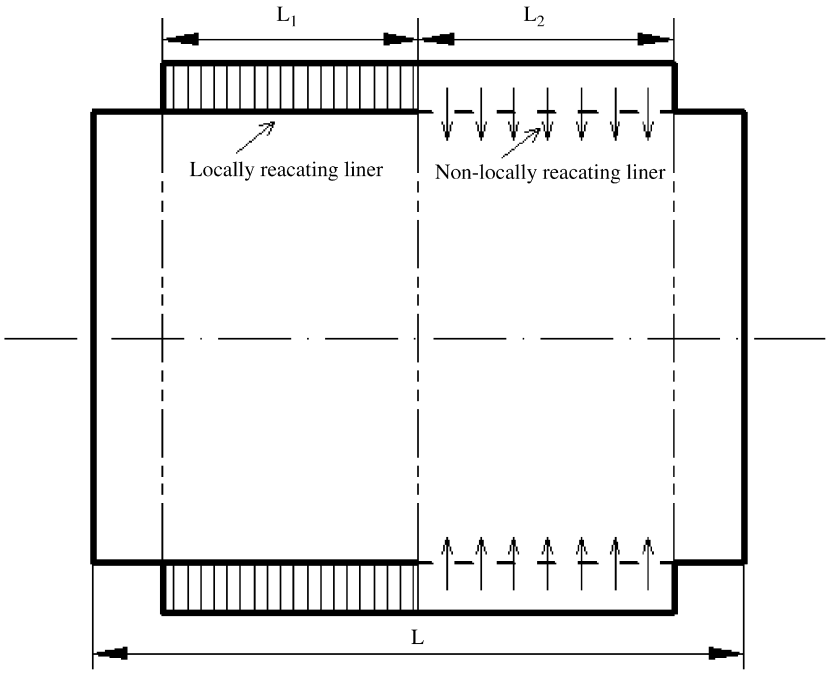

Fig. 14. Sketch of segmented liners.

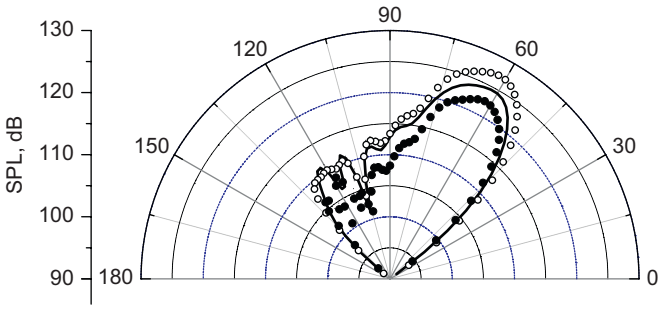

Fig. 15. Sound pressure level at spherical radius 10 m; $M=-0.4$, $T=1.0$ kN, $\omega r_0/c_0=1.22$, $L=r_0=1.0$ m, $r_s/r_0=0.9$, $L_1=L_2=0.4$ m, $Z_1=(2.0, 0)$ ——, local: $L_2=0.4$ m, $Z_2=(0.5, 0.5)$; ○, non-local: $L_2=0.4$ m, $r_1=1.1$ m, $h_t=0.001$ m, $\sigma=0.02$, $a=0.001$, $M_h=0.005$; ●, non-local: $L_2=0.4$ m, $r_1=1.1$ m, $h_t=0.001$ m, $\sigma=0.02$, $a=0.001$, $M_h=0.05$.

may lead to a more appropriate tool for the acoustic liner optimization than a usual procedure due to more design degrees of freedom.

4. Conclusions

It is noted that a non-locally reacting liner with adjustable wall impedance may play some role in future techniques related to hybrid active/passive control of aeroengine noise. However, there are few models available to include the effect of non-locally reacting liner on the prediction of sound radiation from a finite duct in current literatures. This paper presents a unified model to study the effect of both locally and non-locally reacting liners on the acoustic fields generated by fan blade rotating sources. Various numerical experiments show that this model can not only give a good agreement with existing results for locally reacting liner but also has a capability to predict the sound radiation from fan rotating blade sources with an arbitrary combination of locally and non-locally reacting liners, which indeed provides more choices for the preliminary parameter design of optimum liner.

Acknowledgement

This work was supported by NSFC under grants 50736007, 10472009 and 50136010.

References

[1] E. Envia, Fan noise reduction: an overview, NASA TM-2001-210699, 2001.
[2] M.H. Dunn, J. Tweed, F. Farassat, The application of a boundary integral equation method to the prediction of ducted fan engine noise, *Journal of Sound and Vibration* 227 (5) (1999) 1019–1048.
[3] M.K. Myers, M. Kosanchik III, Computation of sound radiation from a fan in a short lined duct, AIAA-97-1711-CP, 1997.
[4] W. Eversman, Turbofan noise propagation and radiation at high frequencies, NASA CR-2003-212323, 2003.
[5] W. Rienstra, W. Eversman, A numerical comparison between the multiple-scales and finite-element solution for sound propagation in lined flow ducts, *Journal of Fluid Mechanics* 437 (2001) 367–384.
[6] Y. Ozyoruk, L.N. Long, Time-domain calculation of sound propagation in lined ducts with sheared flows, AIAA 99-1817, 1999.
[7] Y. Ozyoruk, V. Ahujia, L.N. Long, Time domain simulation of radiation from ducted fans with liners, AIAA 2001-2171, 2001.
[8] X. Li, C. Scemel, U. Michel, F. Thiele, On the azimuthal mode propagation in axisymmetric duct flows, AIAA 2002-2521, 2002.
[9] E. Envia, A.G. Wilson, D.L. Huff, Fan noise: a challenge to CAA, *International Journal of Computational Fluid Dynamics* 18 (2004) 471–480.
[10] M.H. Dunn, F. Farassat, Liner optimization studies using the ducted fan noise prediction code TBIEM3D, AIAA-98-2310, 1998.
[11] F.V. Hutcheson, Advanced modeling of active control of fan noise for ultra high bypass turbofan engines, PhD Dissertation, Virginia Polytechnic Institute and State University, Blacksburg, Virginia, 1999.
[12] P.D. Dean, On the "in-situ" control of acoustic liner attenuation, *Journal of Engineering for Power* 92 (1977) 63–70.
[13] M.S. Howe, On the theory of unsteady high Reynolds number flow through a circular aperture, *Proceedings of the Royal Society of London A* 366 (1990) 299–335.
[14] I.J. Hughes, A.P. Dowling, The absorption of sound by perforated linings, *Journal of Fluid Mechanics* 218 (1990) 299–335.
[15] M.S. Howe, *Acoustics of Fluid– Structure Interactions*, Cambridge University Press, 1998, pp. 317–430 (Chapter 5).
[16] H. Zhao, X. Sun, Active control of wall acoustic impedance, *AIAA Journal* 37 (7) (1999) 825–831.
[17] X. Sun, X. Jing, H. Zhang, Effect of grazing–bias flow interaction on acoustic impedance of perforated plates, *Journal of Sound and Vibration* 254 (3) (2002) 557–573.
[18] X. Jing, X. Sun, Sound-excited flow and acoustic nonlinearity at an orifice, *Physics of Fluids* 14 (1) (2002) 268–276.
[19] X. Sun, X. Jing, H. Zhao, Control of blade flutter by smart casing treatment, *AIAA Journal of Propulsion and Power* 17 (2) (2001) 248–255.
[20] X. Jing, X. Sun, Wall thickness influence on the impedance of perforated plates with bias flow, *AIAA Journal* 38 (9) (2000) 1573–1578.
[21] J.D. Eldredge, A.P. Dowling, The absorption of axial acoustic waves by a perforated liner with bias flow, *Journal of Fluid Mechanics* 485 (2003) 307–335.
[22] J.D. Eldredge, On the interaction of higher duct modes with a perforated liner system with bias flow, *Journal of Fluid Mechanics* 510 (2004) 303–331.
[23] J.M. Tyler, T.G. Sofrin, Axial compressor noise studies, *Society of Automotive Engineering Transactions* 70 (1962) 309–332.
[24] W. E. Zorumski, Acoustic theory of axisymmetric multisection ducts, NASA TM-R-419, 1974.
[25] M. Namba, K. Fukushige, Application of the equivalent surface source method to the acoustics of duct systems with non-uniform wall impedance, *Journal of Sound and Vibration* 73 (1) (1980) 125–146.
[26] L. Huang, A theoretical study of duct noise control by flexible panels, *Journal of the Acoustical Society of America* 106 (4) (1999) 1801–1809.
[27] W.E. Zorumski, Generalized radiation impedance and reflection coefficient of circular and annular ducts, *Journal of the Acoustical Society of America* 54 (1973) 1667–1673.
[28] D.L. Lansing, W.E. Zorumski, Effects of wall admittance changes on duct transmission and radiation of sound, *Journal of Sound and Vibration* 27 (1973) 85–100.
[29] B. Soenarko, A boundary element formulation for radiation of acoustic waves for axisymmetric bodies with arbitrary boundary conditions, *Journal of the Acoustical Society of America* 93 (1993) 631–639.
[30] A.F. Seybert, B. Soenarko, F.J. Rizzo, D.J. Shippy, A special integral equation formulation for acoustic radiation and scattering for axisymmetric bodies and boundary conditions, *Journal of the Acoustical Society of America* 80 (1986) 1241–1247.
[31] W. Wang, N. Ataun, J. Nicolas, A boundary integral approach for acoustic radiation of axisymmetric bodies with arbitrary conditions valid for all wave numbers, *Journal of the Acoustical Society of America* 101 (3) (1997) 1468–1478.
[32] W. Koch, Attenuation of sound in multi-element acoustically lined rectangular ducts in the absence of mean flow, *Journal of Sound and Vibration* 73 (1) (1977) 125–146.
[33] M.E. Goldstein, *Aeroacoustics*, McGraw-Hill International Book Company, New York, 1976, pp. 1–66 (Chapter 1).
[34] M.K. Myers, Radiation of sound from a point source in a short duct, in: C.K.W. Tam, J. Hardin (Eds.), Second CAA Workshop on Benchmark Problems, NASA CP-3352, 1997, pp. 19–26.
[35] M.H. Dunn, TBIEM3D—a computer program for predicting ducted fan engine noise, NASA CR-97-206232, 1997